

## **Isothermal decomposition of austenite in presence of martensite in advanced high strength steels**

### **A review**

Dhara, Sharmistha; van Bohemen, Stefan M.C.; Santofimia, Maria J.

#### **DOI**

[10.1016/j.mtcomm.2022.104567](https://doi.org/10.1016/j.mtcomm.2022.104567)

#### **Publication date**

2022

#### **Document Version**

Final published version

#### **Published in**

Materials Today Communications

#### **Citation (APA)**

Dhara, S., van Bohemen, S. M. C., & Santofimia, M. J. (2022). Isothermal decomposition of austenite in presence of martensite in advanced high strength steels: A review. *Materials Today Communications*, 33, Article 104567. <https://doi.org/10.1016/j.mtcomm.2022.104567>

#### **Important note**

To cite this publication, please use the final published version (if applicable).  
Please check the document version above.

#### **Copyright**

Other than for strictly personal use, it is not permitted to download, forward or distribute the text or part of it, without the consent of the author(s) and/or copyright holder(s), unless the work is under an open content license such as Creative Commons.

#### **Takedown policy**

Please contact us and provide details if you believe this document breaches copyrights.  
We will remove access to the work immediately and investigate your claim.



# Isothermal decomposition of austenite in presence of martensite in advanced high strength steels: A review

Sharmistha Dhara<sup>a,\*</sup>, Stefan M.C. van Bohemen<sup>b</sup>, Maria J. Santofimia<sup>a</sup>

<sup>a</sup> Delft University of Technology, Delft, The Netherlands

<sup>b</sup> Tata Steel, IJmuiden, The Netherlands

## ARTICLE INFO

### Keywords:

Pre-existing martensite

Isothermal transformation

Bainite

Advanced high strength steels

## ABSTRACT

The development of the quenching and partitioning (Q&P) process has prompted an interest in the process of isothermal transformation in presence of a pre-existing phase such as martensite. The presence of prior martensite is known to accelerate the overall kinetics of bainite formation, both in the 1-step and 2-step Q&P process. The underlying mechanisms behind this phenomenon are not fully understood. Also, the nature of the isothermal product (isothermal martensite and/or bainite) formed in presence of prior martensite seems to differ according to the thermodynamic and kinetic conditions. For certain thermodynamic conditions, depending on alloying, isothermal martensite may also form in the temperature range just above and below  $M_s$ . In the event that both bainite and isothermal martensite formation are thermodynamically allowed, the competition in kinetics determines the observed transformation product. The effect of martensite on the subsequent isothermal transformation is reviewed with a focus on the nature of the transformation products and kinetics. In that context, the kinetics of the isothermal transformation in presence of other prior phases such as polygonal ferrite and bainite are also compared and discussed, together with the possible mechanisms behind the acceleration of the transformation kinetics. Guidelines for further investigation are also proposed.

## 1. Introduction

The ever increasing demand for safer and lighter vehicles has prompted the steel community to develop steels with higher strength compared to conventional high strength steel grades. This led to the development of advanced high strength steels (AHSS), and ultra-high strength steels (UHSS). The combination of high strength and good ductility is achieved by ultrafine-grained microstructure, often including a mixture of softer (e.g. ferrite, retained austenite) and harder phases (e.g. martensite, bainite). The softer phases account for the desired ductility, whilst the strength is imparted by the comparatively harder phases. Retention of austenite is often desired in such steels, as besides ductility, it may also improve strength through the transformation induced plasticity (TRIP) effect, originated from the deformation-induced transformation of the retained austenite to martensite [1]. In most of the processing strategies, austenite is retained by its thermodynamic stabilisation through carbon enrichment [2,3]. However, austenite retention is also possible by the diffusion of substitutional elements such as Ni [4], as in case of stainless steels and Mn [5] as in medium manganese steels.

Owing to their attractive properties, recent research on the 3rd generation AHSS is focused on steels such as medium manganese steels [6,7], carbide-free bainitic (CFB) steels [8–11] and quenching and partitioning (Q&P) steels [3,12,13]. All three kind of steels may exhibit a strength of more than 1200 MPa with impressive formability properties. Medium manganese steels may contain 3–12 wt% Mn and exhibit martensite after both hot and cold rolling stages [6]. Generally, the processing of these steels involve an inter-critical batch-annealing step to obtain a controlled volume fraction of retained austenite stabilised by Mn partitioning [6]. In contrast, in the case of CFB and Q&P steels, the retained austenite is stabilised through carbon enrichment.

The heat treatment strategies for the CFB steels involve an isothermal heat treatment between the  $B_s$  (Bainite start) and  $M_s$  (Martensite start) temperatures (Fig. 1a), generally at a temperature closer to the  $M_s$ , so that fine plates of the bainite could form because of the lower transformation temperature, albeit avoiding the martensite formation [8–10]. Bainite formation during the isothermal treatment allows the excess carbon to be partitioned into austenite until the carbon content of the remaining austenite reaches the concentration given by the  $T_0$  curve [14,15]. In the conventional 2-step Q&P process [3,12,13], the steel is

\* Corresponding author.

E-mail address: [s.dhara@tudelft.nl](mailto:s.dhara@tudelft.nl) (S. Dhara).

<https://doi.org/10.1016/j.mtcomm.2022.104567>

Received 14 July 2022; Received in revised form 13 September 2022; Accepted 26 September 2022

Available online 28 September 2022

2352-4928/© 2022 The Authors. Published by Elsevier Ltd. This is an open access article under the CC BY license (<http://creativecommons.org/licenses/by/4.0/>).

quenched to a temperature between the  $M_s$  and  $M_f$  (Martensite finish) temperature after a full austenitisation to form a relatively high fraction of athermal martensite, typically between 75% and 90% (Fig. 1b). Such a high fraction of martensite ensures that the remaining austenite is adequately stabilised after an isothermal step, known as the partitioning treatment, at an elevated temperature. During the partitioning stage the carbon from the supersaturated martensite partitions into the austenite, leading to its stabilisation. In the event that the austenite is not sufficiently stabilised, it may partly transform to fresh martensite during final cooling to room temperature. The formation of fresh martensite is however undesired owing to its negative consequences in the mechanical properties. The hard fresh martensite has a high phase contrast with the softer tempered martensite and/or bainite and therefore it is detrimental for the local formability properties of the steel.

The possibility of combining the microstructures observed in CFB and Q&P steels has been discussed by Santofimia et al. [16] and could be termed as an hybrid approach of Q&P and CFB. An example of the heat treatment route proposed in [16] is shown in Fig. 1c. Compared to conventional Q&P, the quench-stop temperature is higher to form an athermal martensite fraction in the range of 30–70%. Then the steel is isothermally heat treated at an elevated temperature within the bainite range, in order to allow bainite formation. Additionally, the prior athermal martensite will be tempered during the isothermal treatment. Therefore, the austenite has the opportunity to become enriched in carbon through its partitioning from both tempering of martensite and formation of bainite and hence, the enhanced stabilisation of austenite will minimize the formation of fresh martensite in the final cooling step. In principle, the carbon partitioning process from martensite may counteract the bainite formation as the later can be retarded by the carbon-enrichment of austenite. In contrast, an acceleration in the overall bainite formation kinetics in the presence of martensite has been observed by many researchers [17–24]. However, the dominating mechanism for this acceleration has not been elucidated yet. Instances of acceleration of bainite formation kinetics below the  $M_s$  temperature in lean medium manganese steels was also reported [25]. However, it should be noted that the chemical composition of such steels is quite similar to CFB and Q&P steels, allowing occurrence of bainite formation near the  $M_s$ . The proposed mechanisms for acceleration of bainite kinetics include the introduction of new interfaces and transformation strains in the untransformed austenite as a result of prior martensite formation [17,21–23]. The possible variations in the local carbon concentration also may influence the subsequent isothermal transformation.

The proposed hybrid route will reduce the annealing time compared to normal CFB processing. In comparison to conventional Q&P, the opportunity of tuning the austenite stabilisation by both bainite formation and martensite tempering may have advantages for reaching a better high strength-ductility combination.

In this paper we review various investigations involving isothermal transformation of austenite in the presence of prior martensite in steels.

The martensite in the present case is athermal in nature and will be referred as “prior martensite” or “martensite” throughout the text. The discussion is focused on the transformation of austenite near the  $M_s$  temperature considering the possible phases/aggregates that may form during the isothermal treatment in the presence of prior martensite. The isothermal transformation kinetics and possible mechanisms are also discussed in this overview.

## 2. Austenite decomposition near the $M_s$ temperature

### 2.1. Martensite formation

The austenite in steel may transform to martensite, when the steel is cooled below the martensite start ( $M_s$ ) temperature with a cooling rate sufficiently high to avoid other solid-state transformations, such as ferrite. The martensitic transformation in steel is regarded as a diffusion less shear transformation [26]. Three different modes of martensitic transformation are found in the literature [26,27]:

1. Athermal mode: In the athermal mode of transformation, the volume fraction of martensite depends on the temperature. The transformation proceeds by formation of new units with the lowering of temperature below the  $M_s$  temperature. In steels, the martensitic transformation is “athermal”, and the transformation kinetics is often too fast to allow experimentally accessible time scale observation [26,27].
2. Burst mode: In this mode, the martensitic transformation starts off abruptly and a certain quantity of martensite is formed in a single event (or “burst”) within a small temperature interval, generally observed in Fe-Ni and Fe-Ni-C alloys below the athermal  $M_s$  temperature [27,28]. The burst mode is regarded as a result of autocatalysis in extreme form, triggered by the large stress field associated with the formation and growth of the initial plates [26,27].
3. Isothermal mode: In this mode, the transformation proceeds by formation of new units as a function of time when the steel is kept at a temperature below a critical temperature  $M_{si}$ , the upper temperature limit for the formation of isothermal martensite [29].  $M_{si}$  is different from the  $M_s$  temperature, and can be higher or lower than the start of the athermal transformation. In the former case, i.e. in the absence of primary athermal martensite formed as a result of cooling to the isothermal temperature, the reaction rate is slow at the start and attains a maximum value at a certain volume fraction, followed by a slower rate at the end [27]. The reaction rate and the fraction transformed increase with decreasing temperature [27]. Maximum reaction rate may be reached at the beginning of the transformation in presence of a small fraction of primary athermal martensite [27]. Many researchers proposed that the kinetic behaviour of isothermal martensite in Fe alloys with high C or alloy contents (Mn, Ni and Cr) follows C-shaped curves similar to diffusional transformations in steel [30–33].

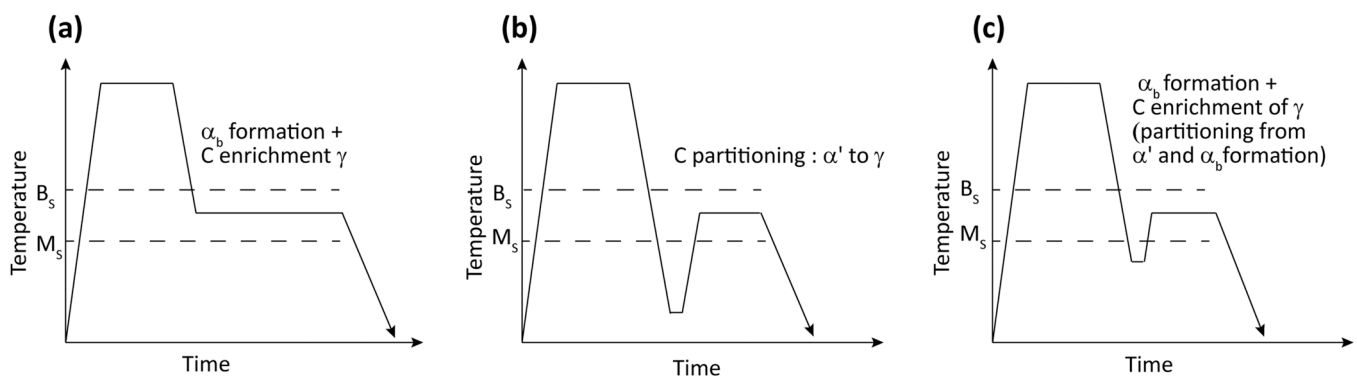


Fig. 1. Processing conditions for (a) CFB steels (b) Q&P steels and (c) present discussion. ( $\alpha_b$ : bainite,  $\alpha'$ : martensite and  $\gamma$ : austenite).

In low-alloyed steels athermal martensite is generally observed. Instances of isothermal martensite formation have been reported in hypereutectoid steel [34–37]. All the three modes of transformation can be observed in Fe-Ni alloys. In fact, it is common for the Fe-Ni alloys to form martensite in athermal or burst mode before it reached the critical temperature to form martensite in the isothermal mode [27,38].

The athermal martensitic transformation has been extensively studied in the literature [27,34,39–42]. It is well established that martensite grows by a displacive, shear mechanism. The nucleation is believed to start at the microstructural defects by means of spontaneous dissociation of dislocations present in the parent phase [42]. The transformation accompanies a volume change and as a result of the plastic accommodation associated with the volume change and shear strain, dislocations are generated in the surrounding austenite matrix [43–45]. In this process, the remaining austenite may become mechanically stabilised when the stress driving the glissile interface associated with the transformation becomes equal to that generated by the dislocation debris hindering the movement [46].

The progress of the athermal martensite transformation can be described by the Koistinen and Marburger (KM) equation [39,40],

$$f = 1 - \exp[-\alpha_M(T_{KM} - T)] \quad (1)$$

Here,  $f$  is the volume fraction of martensite transformed,  $\alpha_M$  is the rate parameter and  $T_{KM}$  is the model start temperature for martensite. The rate parameter depends on the composition [47]. The fit parameter  $T_{KM}$  is about 10–30 °C lower than the experimental  $M_s$  temperature [47], depending on the alloying and the austenitising conditions. The  $M_s$  temperature is mainly influenced by the chemical composition and in particular the austenite carbon concentration [48]. By plotting the experimental data available from the literature, van Bohemen has demonstrated that the  $M_s$  temperature is exponentially related to the carbon content in the range of 0.17–1.8 wt% C [48]. Experiments with different austenitising temperatures have demonstrated that the  $M_s$  temperature also depends on the austenite grain size [49–51].

During an isothermal stop between the  $M_s$  and  $M_f$  temperature, part of the remaining austenite may become stabilised as it becomes enriched in carbon [4,26,52,53]. This phenomenon designated as thermal stabilisation impacts the available fraction of austenite to be transformed into martensite upon resumed cooling after the isothermal stop. Despite the thermal stabilisation, evidences of austenite decomposition at lower temperatures were reported in investigations concerning long isothermal holding times below the  $M_s$  temperature. Possibilities of bainite and isothermal martensite formation were suggested to explain the observations during such isothermal stops in these early investigations [17–19,54,55].

## 2.2. Phase transformations following isothermal holding after martensite formation

Some of the earliest literature about the isothermal decomposition of austenite below the  $M_s$  temperature date back to 1940 s. These initial investigations explored the phase transformations that could occur within the martensite formation range. Most of these early investigations were concentrated on high carbon steels, while the comparatively lower carbon containing steels have been studied more recently. Hereafter the discussion has been presented in two parts, based on the carbon concentration of the investigated steels in the literature.

### 2.2.1. High-C steels

Howard and Cohen (1948) were probably the first researchers to systematically study the austenite decomposition below the  $M_s$  temperature and compare it with the transformation just above the  $M_s$  [17]. They identified athermal martensite and units of bainitic ferrite in steels heat treated below the  $M_s$  in their study concerning a wide range of steel compositions (0.75–1.35 wt% C) [17]. Based on the similarity of the isothermal transformation kinetics below the  $M_s$  with the bainite

kinetics above the  $M_s$  as well as from microstructural evidence, they identified the isothermal product below the  $M_s$  as bainite [17]. Additionally, they observed another product in the 1.35 wt% C steel isothermally treated between 160 °C and  $M_s$  (105 °C), appearing as “long, thin plates or needles” with the “dark etching characteristics of bainite”, but different from bainite [17]. In the 1980 s, Oka and Oka-moto further investigated the product, identifying it to be a mixture of various morphologies of isothermal martensite and/or bainite [35–37].

Schaaber (1955) suggested formation of both isothermal martensite and bainite during isothermal treatments near the  $M_s$ , in a range of steel compositions (0.4 – 1.1 wt% C) [55]. The reported isothermal transformation kinetics of the 0.89 C-0.30Mn-0.36Si-1.28Cr steel followed a two-stage curve for the isothermal temperature of 215 °C marked as I and II in Fig. 2 [55]. Schaaber theorised that initially isothermal martensite (stage I in Fig. 2) was formed followed by bainite formation at the second stage [55]. However, few aspects should be considered in this investigation. First of all, the  $M_s$  was not mentioned, making the interpretations difficult. Also the conclusions were based solely on the dilatometer measurements, without further verifications using methods such as metallography. The possible two stage kinetics can be distinguished for the isothermal temperature of 215 °C only. Considering that the steel composition is similar to the 100Cr6 bearing steel, it is important to note that no indications of such two stage isothermal transformations could be observed in the TTT diagrams of 100Cr6 [56]. The dilatometers used in such earlier investigations were different from the modern day equipment with high precision in temperature control. Assuming that the experimental set up in Schaaber’s investigation was similar to Davenport and Bain (1930) [57], the sample temperature possibly decreased slowly during the initial few minutes after the transfer to the dilatometer from the salt bath. Formation of athermal martensite is therefore possible during the cooling with suitable conditions. Because of the slow cooling rate, the kinetics of the athermal martensite would then appear as “isothermal”. This could be true in most of the earlier investigations involving heat treatments of relatively large samples, and hence large heat capacity, whereby one or multiple transfers were needed from one furnace/ salt bath to another furnace/salt bath. Although the furnaces and salt baths were in thermal equilibrium, the possibility of undesired transformation happening during the transfer and hence experimental artefacts could not be ruled out.

Edwards (1970) also reported two transformation products termed as type I and II, formed during the isothermal transformation both above and below the  $M_s$ , in a 1.44 wt% C steel [54]. The “Type II” product was identified as ferrite containing carbide ( $Fe_3C$ ) precipitates whilst the “Type I” product contained either high dislocation density or arrays of

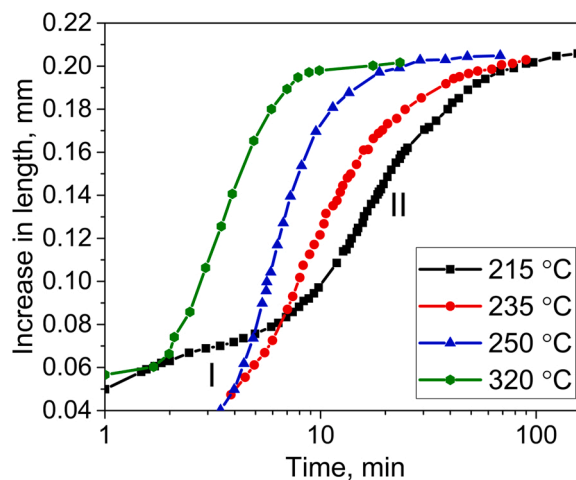


Fig. 2. Increase in change in length with time at various isothermal transformation temperatures in a 0.89 C-0.30Mn-0.36Si-1.28Cr (wt%) steel [55].

dislocations along with epsilon carbide ( $\text{Fe}_{2.4}\text{C}$ ) precipitates [54]. Based on the morphology and habit plane analysis Edwards concluded that the “Type I” and “Type II” products were isothermal martensite and lower bainite, respectively [54] and therefore agreed with Schaaber’s speculation. In some cases, the carbides in the “Type II” product were nucleated at the austenite/ferrite interface and grown into the ferrite, giving it a “central mid-rib” feature (Fig. 3a) [54].

Similar investigations of austenite decomposition near the  $M_s$  were performed by Oka and Okamoto (1985–1988) in a range of hypereutectoid steels (0.85 – 1.80 wt% C), who attempted to identify the isothermal product(s) as well as its relationship with the observed kinetics [35–37]. They observed an isothermal product equivalent to that described by Howard and Cohen as “long, thin plates or needles with a dark etching characteristics of bainite” in all the alloys and identified its three different morphologies using TEM. A “thin-plate like” morphology (Fig. 3c) was termed as “thin-plate isothermal martensite” (TIM) [37]. The other two morphologies featured a central “mid-rib”, shown in Fig. 3b and d [35–37]; one of those (Fig. 3b) resembled the lower bainite morphology previously observed by Edwards [54] as in Fig. 3a. Oka and Okamoto described it to be a combination of lower bainite and isothermal martensite, and named it as “lower bainite with midrib” (LBm) [37]. The other morphology with the “mid-rib” (Fig. 3d) was termed as “leaf-like isothermal martensite” (LIM) and reported to consist of TIM at the “mid-rib” region and isothermal martensite along the periphery [37]. The TIM and LIM were only observed in 1.45–1.80 wt% C alloys, whilst LBm was observed in all the compositions (0.85–1.80 wt% C alloys) [37]. According to their investigation, both the  $M_s$  and  $M_{si}$  depend on the carbon composition of the steels [37]. They observed that the  $M_{si}$  is considerably higher than the  $M_s$  (difference of  $\sim 90^\circ\text{C}$ ) for 1.45 and 1.80 wt% C steels in contrast to the similar  $M_{si}$  and  $M_s$  for the steels with 0.85 and 1.10 wt% C (difference of  $\sim 35^\circ\text{C}$ ) [37]. They reported difficulty in recognising the TIM and LIM in lower carbon alloys due to the  $M_s$  being close to the  $M_{si}$  [37]. Oka and Okamoto identified the isothermal martensite based on the crystallographic data from their TEM observations, its habit plane being close to that of thin-plate athermal martensite in Fe-Ni-C and Fe-Al-C alloys as compared to lower bainite in hypereutectoid steels [35]. They also showed that the habit plane analysis satisfied the theoretical predictions using the

phenomenological theory of the martensitic transformation [35]. Therefore the athermal and isothermal form of martensite are crystallographically similar, although there are some differences in morphology. For example, Edwards observed the presence of twins in tempered athermal martensite plates, which were not present in the isothermal martensite they identified [54]. It therefore seems difficult to distinguish isothermal martensite from athermal (tempered) martensite in carbon steels without the use of high-end characterisation tools like TEM.

As opposed to the previous investigations [17,55], Oka and Okamoto did not report bainite to form below the  $M_s$ , but admitted difficulty in identifying the TIM and LIM in their lower carbon steels (0.85 and 1.10 wt% C) and suggested co-existence of LBm and athermal martensite [37]. They observed bainite formation at the athermal martensite/austenite interface in the 1.80 wt% C steel quenched and treated at an isothermal temperature above the  $M_s$  [36]. But they did not mention whether the LBm could be observed at such athermal martensite/austenite interfaces. It could be possible that the formation of the isothermal martensite was more pronounced in higher carbon steel compositions. Implying that the bainite kinetics are expected to be much slower in the 1.45–1.80 wt% C steels compared to that in the lower carbon steels (0.85 wt% and 1.10 wt% C steels), the isothermal holding time for the higher C steels was possibly insufficient to form bainite below the  $M_s$  temperature. In presence of athermal martensite and at a higher isothermal temperature above  $M_s$ , the bainite formation kinetics was accelerated, which is in agreement with the results reported by Steven and Haynes in the 1950 s [58].

In a more recent work, Toji et al. (2016) investigated the effect of Si on the bainite kinetics in the presence of prior athermal martensite in a 1.1 C - 3Mn, wt% steel with varying Si, using the Q&P treatment [24]. Interestingly, they did not report isothermal martensite formation in their investigation [24]. Their isothermal heat treatment was performed above the  $M_s$  temperature after forming athermal martensite during the initial quench [24]. It is to note that most of the above mentioned previous investigations concerned isothermal heat treatments at the quenching temperature. The possibility of isothermal martensite formation seems to be related to the steel composition and the isothermal treatment conditions. Although Edwards also observed isothermal

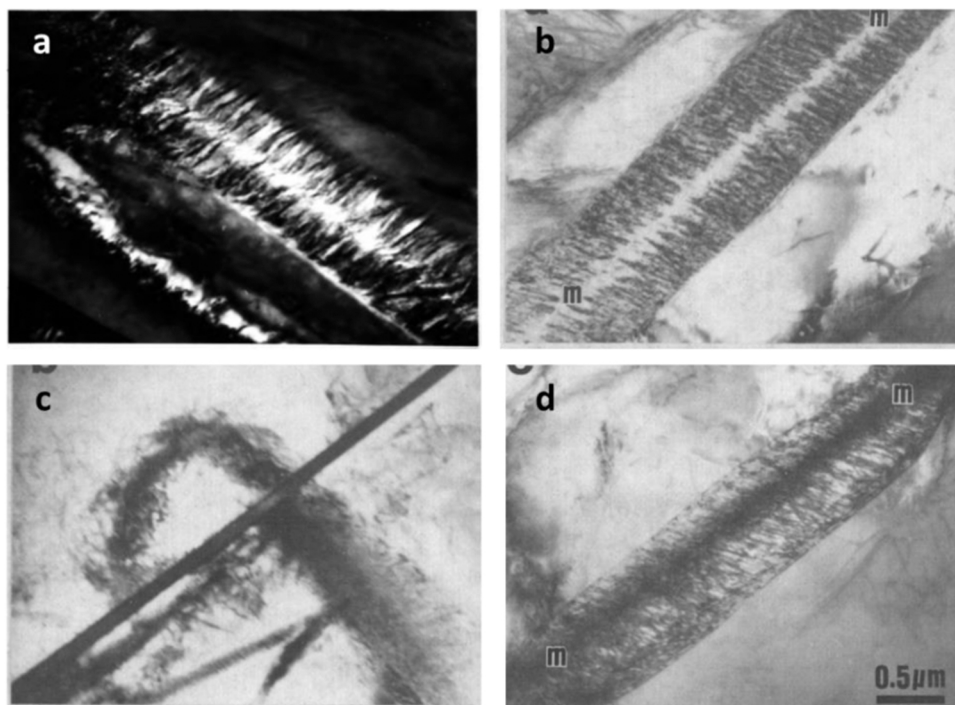


**Fig. 3.** TEM bright-field analysis of the following microstructural features: (a) 1.44 wt% C steel, isothermally transformed at  $120^\circ\text{C}$  for 150 h, showing “carbide platelets” nucleated at the edge of  $\alpha$  plate and grown into it, giving it a “central mid-rib” appearance (55,000X), work by Edwards [54]. 1.80 wt% C steel isothermally transformed at different conditions, illustrating microstructural features identified by Oka and Okamoto. (b) Lower bainite with midrib. (c) Thin-plate isothermal martensite. (d) Leaf-like isothermal martensite [37]. The scale bar in Fig. 3d is also applicable for Fig. 4b and c.



martensite formation above the  $M_s$  temperature ( $M_s$ : 92 °C) up to 130 °C (without prior martensite formation) followed by bainite [54], it seems plausible that the thermodynamic and kinetic conditions were suitable for that steel to form isothermal martensite first.

In summary, most of the investigations in high C steels reported isothermal martensite as well as bainite as the products of the isothermal transformation in presence of prior martensite. Oka and Okamoto (1986) have shown the conventional lower bainite may transition to lower bainite with midrib (LBm) below a certain temperature [36]. The transition temperature could be assumed as the isothermal martensite start temperature,  $M_{Si}$ , since they suggested that the formation of TIM is the first step in that transition. In a later article (1988) they further suggested the  $M_{Si}$  could also be related to the start of the swing-back phenomenon observed in high carbon steels, referring to the formation of TIM as the reason for the phenomenon, as it will be discussed in Section 2.3 [37]. Assuming that  $M_{Si}$  depends on the composition controlling the thermodynamics and that the formation of isothermal martensite follows a C-curve kinetics [27], it is possible that there is a competition between the kinetics of isothermal martensite and bainite. As a result, observation of isothermal martensite can only be possible if its kinetics is faster than that of bainite. For an interrupt temperature  $T_{hold}$  below the  $M_s$ , the bainitic transformation can in principle take place as the  $B_s$  temperature is generally higher than the  $M_s$ . However, as mentioned above, on the event that the  $T_{hold}$  is below  $M_{Si}$ , the possible observation of bainite depends on its kinetics since its formation has to compete with the isothermal martensite. Also, the mechanical stabilisation of austenite will be an important factor controlling the kinetics of both of these reactions.

## 2.2.2. Medium- and low-C steels

The recent development of the Q&P process [3,12] has renewed the discussion about the transformation of austenite below the  $M_s$  temperature. Understanding the phase transformations near the  $M_s$  temperature in the presence of martensite could assist in austenite stabilisation, one of the key components of the Q&P process. In recent investigations (2008–2016) [20,22,59–65], complimentary characterisation

techniques such as dilatometry, electron microscopy and X-ray diffraction (XRD) were utilised for studying the microstructural features and kinetics of the isothermal product formed in the presence of prior martensite. Many researchers observed a dilatation during the isothermal holding after the formation of a certain amount of martensite, indicating a phase transformation from austenite to a body centred cubic (bcc) structure [20,59,61]. It is important to note that these investigations were performed with various steel compositions (C varying between 0.16 and 0.66 wt%, see Table 1 for composition details). Since the tempering of martensite leads to volume contraction [59,66], the investigators alternatively suggested that the observed dilatation could be related to the formation of bainite and/or isothermal martensite as both reactions would result in volume expansion. Upon observation of the morphological and kinetics resemblance of the isothermal product with that of the lower bainite formed above the  $M_s$  and arguing that the isothermal martensite formation is primarily observed in hypereutectoid steels [20,59,61], all these researchers independently came to the conclusion that the isothermal product formed below the  $M_s$  was bainite.

Kolmskog et al. (2012) used in situ synchrotron X-ray diffraction and laser scanning confocal microscopy, for investigating the initial stage of austenite decomposition below the  $M_s$  temperature [67]. They observed the formation of two different phases distinguished by their growth rates ( $\sim 7 \mu\text{m/s}$  and  $3 \text{ mm/s}$ , respectively) and suggested that the fast-growing unit was martensite whilst the slower growing unit was bainite [67]. As the investigated time duration also included the quenching stage, it could be assumed that the martensite was formed during the quenching stage followed by bainite at the initial isothermal holding stage.

Clearly, the above investigations on hypoeutectoid steels indicated bainite as the isothermal product formed in the presence of martensite. However, detailed characterisation of the isothermal product was still missing in these investigations. In an effort to distinguish the isothermal product, Kim et al. compared its morphology with that of athermal martensite and lower bainite (formed above the  $M_s$ ) in a 0.2 C-1.5Mn-1.5Si (wt%) steel [63–65]. They reported that the isothermal product

**Table 1**

Composition,  $M_s$  temperature, isothermal transformation (IT) range and isothermal product (IP) formed in presence of martensite, various studies.

Authors (Year)	Composition (wt%)				$M_s$ (°C)	IT range (°C)	Time	Identified IP
	C	Mn	Si	other				
Howard and Cohen (1948)[17]	0.75–1.35	–	–	–	250–105	80–300	0–100 h	B
Elmendorf (1944)[19]	0.66	0.78	0.22	–	200–260 (approx.)	315–482	$\sim 1000$ s	B
	0.80	0.87	0.23	–				
	0.91	0.46	0.23	–				
	0.64	0.61	0.20	0.25Mo				
	0.89	0.30	0.36	1.28Cr				
Schaaber (1955)[55]	1.08	0.41	0.29	1.43Cr	–	110–320	–	B+IM
	0.36	1.71	0.33	0.16Cr				
	0.43	1.82	0.22	0.08Cr				
	0.82	0.82	1.86	–				
	0.77–1.2	–	–	–				
Radcliffe and Rollason (1959)[18]	0.77–1.2	–	–	–	264–180	186–450	–	B
Edwards (1970)[54]	1.44	0.38	0.12	0.020Ni-0.165Cr	93	70–130	0.5–350 h	B+IM
Oka and Okamoto (1985–88)[35–37]	0.85	< 0.01	–	–	273	167–328	–	TIM, LIM, LBm <sup>#</sup>
	1.10	–	–	–	231	–	–	–
	1.45	–	–	–	189	–	–	–
	1.80	–	–	–	174	–	–	–
	0.66	0.69	0.30	–	264	220–300	100–7200 s	B
van Bohemen et al. (2008)[59]	0.15	1.50	1.42	–	393	300–550	–	isothermal product*
	0.15	2.50	0.30	–	367	–	–	–
	0.15	2.32	0.50	0.50Al	410	–	–	–
	0.15	2.00	0.30	0.80Al	400	–	–	–
	0.2	2.0	1.5	0.6Cr	395	290–450	10–1000 s	B+IM
Pinto da Silva et al. (2014)[20]	0.16	1.6	0.4	0.8Cr-0.3Mo	420	450–100	1 h	B
Navarro-López et al. (2016)[22]	0.2	3.51	1.52	0.04Al-0.25Mo	320	270–370	1 h	B
Samanta et al. (2016)[61]	0.32	1.78	0.64	1.20Co	355	210	60 s	B

B: bainite, IM: isothermal martensite

\*features are specific to neither bainite nor martensite

<sup>#</sup>TIM: thin-plate isothermal martensite, LIM: leaf-like isothermal martensite, LBm: lower bainite with midribs

featured wider laths (2–3  $\mu\text{m}$ ) compared to the laths observed in athermal martensite (0.5  $\mu\text{m}$ ) [63]. The lower bainite constituents (width: 1  $\mu\text{m}$ ) were reported to have curved boundaries [63] in contrast to the isothermal product exhibiting wavy or ledged boundaries as shown in Fig. 4a [64,65]. Both the athermal martensite and isothermal product were reported to exhibit multi-variant carbide precipitates inside the constituent units [65]. Additionally, they noticed morphological differences in the retained austenite present in the three products. In lower bainite, both blocky and thin-film morphologies were reported in contrast to the only thin-film morphology in athermal martensite and the isothermal product. From these observations Kim et al. reasoned that the isothermal product showed more similarities with the athermal martensite compared to the lower bainite. They proposed that these units grew by thickening of the already formed laths during the isothermal treatment, further suggesting that the wavy boundaries were a result of the dislocation interaction during the lateral advancement of the laths [65].

Similar features exhibiting wavy boundaries were also observed by Somani et al. (2014) [60] and Navarro-López et al. (2017) [68] as shown in Fig. 4b and c, respectively. Interestingly the steel compositions and the nature of the heat treatments were somewhat similar in all the three investigations except the isothermal transformation time. Somani et al. [60] associated the products featuring wavy boundaries with isothermal martensite. Similar to Schaaber (Fig. 2) [55], Somani et al. reported two distinct zones in the dilatation vs. time plots (Fig. 5) suggesting the volume expansion at the two different zones related to carbon partitioning and isothermal martensite formation followed by bainite formation [60]. They also proposed that the ferritic units of some of the athermal martensite packets isothermally grew into austenite by the migration of ledges during the isothermal holding. This explanation is not consistent with the conventional viewpoint that the isothermal mode of martensite transformation propagates by the nucleation of new martensite plates [69]. Although the formation of isothermal martensite is probable as evident from the distinct zones observed in the dilatation curve (Fig. 5), it is not clear whether the growth of an athermally formed martensite unit can resume during an isothermal reaction. However, there is another possibility that the units with wavy boundaries are a result of the tempering of the martensite during the isothermal treatment. Upon observing the similar morphology of tempered martensite and the units with wavy boundaries, Navarro-López et al. proposed that the wavy boundaries were created as a result of smaller bainitic ferrite units nucleating and growing from these martensite laths in the form of ledge-like protrusions [68]. Since the characteristics of neither tempered martensite nor the low carbon isothermal martensite formed below the

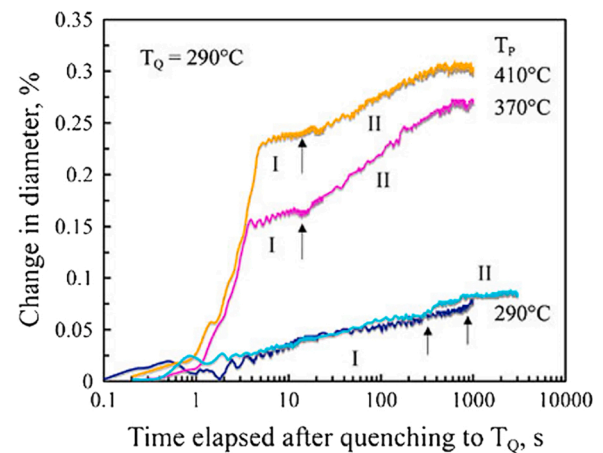


Fig. 5. Change in the specimen diameter with time at various partitioning temperature ( $T_P$ ) after quenching at 290 °C for a 0.2 C-1.5Si-2.0Mn-0.6Cr (wt %) steel [60].

$M_s$  are established in the literature, more detailed investigations are necessary.

It is to note that both Somani et al. [60] and Navarro-López et al. [22, 68] reported bainite formation during the isothermal transformation below the  $M_s$ . However, Kim et al. observed the units with wavy boundaries as the only isothermal transformation product. As there are differences in the isothermal transformation times (Kim et al.: 60 s, Somani et al.: 10–1000 s, and Navarro-López et al.: 3600 s) and from Somani et al.'s suggestion that the bainite forms after the martensitic units with wavy boundaries form, it could be possible that the comparatively shorter transformation time did not allow the bainite formation in the investigation by Kim et al. Interestingly, Navarro-López et al. also reported an acceleration of the bainite kinetics at the start of the isothermal transformation below the  $M_s$  temperature [22]. Such inconsistency of the results therefore displays the complex nature of the isothermal transformation in the presence of martensite and more research is required in order to identify the characteristics of different phases and the sequence of the phase transformations during the isothermal treatment.

In summary, in the case of hypoeutectoid steels, most of the researchers have identified the isothermal transformation product formed in the presence of martensite as bainite, irrespective of the steel carbon composition. Few authors also suggested that the formation of isothermal martensite preceded the bainite formation, mostly in the

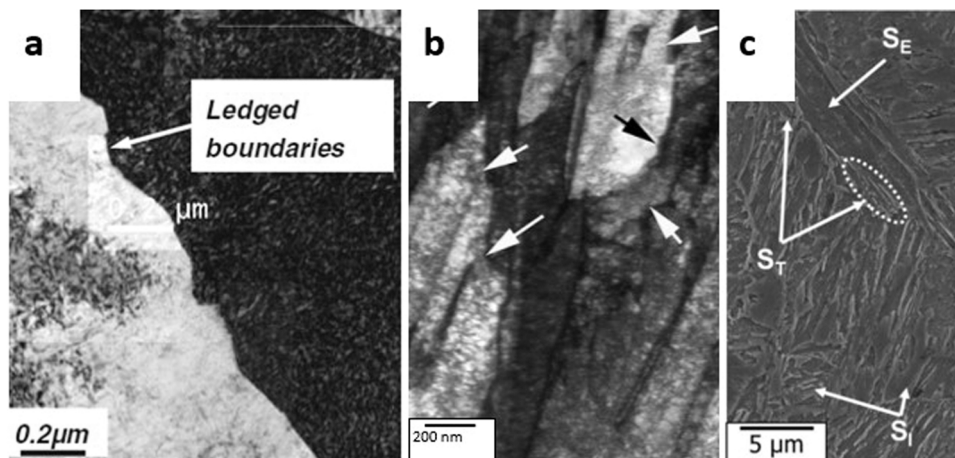


Fig. 4. (a) TEM images showing the wavy/ledged boundaries of the isothermal product formed in a 0.2 C-1.5Mn-1.5Si steel transformed at 390 °C for 100 s [64]; (b) Martensitic laths with wavy boundaries observed under TEM by Somani et al. [60] (c) similar martensitic units with wavy boundaries (marked as  $S_E$ ), observed by Navarro-López et al. [68] under SEM. The other arrowed features  $S_T$  and  $S_I$  are associated with bainite [68].

reports involving high carbon steels. For low carbon steels this sequence of transformation was also proposed by Kim et al. [65] and Somani et al. [60] on the basis of particular microstructural features. However, such morphologies could also potentially form during the tempering of martensite as suggested by Navarro-López et al. [68]. Clearly, a full consensus has not been reached that only bainite forms below  $M_s$  in low carbon steels. Therefore, more investigations are necessary in this area.

Several researchers also studied the effect of the prior athermal martensite formation specifically on the kinetics of bainite formation in steels where bainite was clearly formed during the isothermal treatment [21,24,70–76]. These will be discussed during reviewing the isothermal transformation kinetics. A list of the various investigations involving formation of prior martensite followed by isothermal treatment is presented in Table 1 including information about the composition,  $M_s$  temperature, isothermal transformation range and the reported transformation product(s).

## 2.3. Isothermal transformation kinetics

### 2.3.1. General observations

Howard and Cohen (1948) investigated and compared the isothermal reaction kinetics, above and below the  $M_s$  temperature [17] in hypereutectoid steels. They reported an initial incubation period for the isothermal reaction irrespective of the isothermal transformation temperature being above or below the  $M_s$  [17]. To display the transformation kinetics below  $M_s$  in a TTT diagram, they applied an integrated method to sum up the fractions of athermal martensite and bainite. In other words, the bainite reaction did not start from “zero” position due to the presence of already formed martensite [17]. Howard and Cohen reported an acceleration of the transformation kinetics at the initial stages of the reaction, just below the  $M_s$  compared to that above the  $M_s$  and attributed the accelerated kinetics to the increase in the nucleation site density due to the dislocations generated in the austenite during the martensite reaction as well as formation of martensite/austenite interfaces [17]. They noted the accelerating effect only 20–30 °C below the  $M_s$  and reasoned that although further lowering of the temperature will allow increased martensite volume fraction, the diffusion rate was also expected to be slower at such temperatures, therefore eliminating the accelerating effect of martensite on the bainite formation [17]. Interestingly, for the 1.35 wt% C steel, they observed an accelerated kinetics above  $M_s$ , which they attributed to the formation of a new product, featuring “long, thin plates or needles” in the microstructure [17]. Oka and Okamoto went on to identify this product as thin-plate isothermal martensite, “TIM” [37] (see Section 2.1).

Radcliffe and Rollason (1955) named this accelerating effect near the  $M_s$  as the “swing-back effect” [18]. They reported the “swing-back” below the  $M_s$  temperature for low carbon and eutectoid steels; for hypereutectoid steels the effect was above the  $M_s$  temperature [18]. This statement is somewhat different from the that concluded by Howard and Cohen, who observed the accelerated kinetics above the  $M_s$  only for the 1.35 wt% C steel amongst their investigated compositions of 0.75, 1.12 and 1.35 wt% C steels [17]. According to Radcliffe and Rollason, the phenomenon below the  $M_s$  is well-established and related to the presence of martensite, providing additional potential nucleation sites for the bainite formation, although no reference investigations were indicated [18]. In contrast to the above researchers, Edwards (1970) did not report a considerable decrease of the incubation time in the bainite formation in presence of martensite, although he agreed that the bainite formation could be influenced by the dislocations produced by the martensitic reaction [54]. It is to note that Edwards also reported isothermal martensite as one of the isothermal products [54], but proposed that it did not influence the bainite formation, citing the reason that the dislocations generated during the isothermal martensite formation were not enough to influence the bainite reaction [54], and thereby ignored the possible accelerating effect of the interfaces created as a result of the isothermal martensite formation.

Later Oka and Okamoto (1988) extensively investigated the “swing-back effect” in hypereutectoid steels containing 0.85–1.80 wt% C [37]. As mentioned in Section 2.1, they identified three different microstructural features containing various morphologies of isothermal martensite and/or bainite [36,37]. They suggested that the “swing-back” in the 1.45 and 1.80 wt% C steels was associated with the product TIM; the other two products, LIM and LBm were formed in presence of the TIM [37]. However, in lower carbon steels (0.85 and 1.10 wt% C), they found it difficult distinguishing between the TIM and LIM [37] and therefore, they did not conclude on the reason for the “swing-back” in those compositions.

Amongst the recent investigations, van Bohemen et al. (2008) modelled the kinetics of the isothermal transformation below the  $M_s$  using the Johnson-Mehl-Avrami-Kolmogorov (JMAK) equation [59],

$$f = 1 - \exp(-(kt)^n) \quad (2)$$

Where,  $f$  is the transformed fraction,  $t$  is the time,  $k$  is the rate constant and  $n$  is the Avrami exponent. Using  $n = 2$ , they reported that the  $k$  values above the  $M_s$  temperature follows an Arrhenius type equation [59],

$$k = 58.7 \exp\left(-\frac{Q}{RT}\right) \quad (3)$$

With activation energy  $Q = 43.6$  kJ/mol;  $R$  is the gas constant and  $T$  is the temperature in Kelvin. However, they also pointed out that Eq. 2 overestimated the experimental data to a certain extent when extrapolated below the  $M_s$  temperature (Fig. 6a).

Kim et al. (2012) also used the JMAK equation for fitting the kinetic data, but indicating that the  $n$  value varies with the nature of the transformation [65]. They divided the data in three categories according to the transformation ranges observed in the TTT diagram, namely: bainite (lower bainite formation above  $M_s$ ), swing-back (accelerated lower bainite kinetics in the  $M_s + 50$  °C range) and isothermal transformation below  $M_s$  [65]. It is important to mention that Kim et al. suggested that the isothermal product formed below the  $M_s$  temperature was neither bainitic or martensitic in nature [63,64] (refer section 2.1.2). In their two investigations, Kim et al. reported that the values of both the Avrami constants  $n$  and  $k$  changed sharply as the transformation temperature was lowered below the  $M_s$  [62,65]. An example of such change in the  $k$  parameter is shown in Fig. 6b[65]. They reported comparatively lower activation energies (ranging from 13.5 to 57.3 kJ/mol for various hypoeutectoid steels) required for the isothermal transformation below the  $M_s$  temperature as compared to that required for a diffusion-controlled process [62]. They additionally suggested that the lower activation energies of formation are related to the movement of dislocations formed during the isothermal transformation below the  $M_s$  [62]. It is to note that the activation energy for the bainite formed below the  $M_s$  reported by van Bohemen et al. (43.6 kJ/mol) [59] falls in the range reported by Kim et al. [62,65]. A difference in the trends of the  $k$  parameter between the two investigations could be noted; this could be a result of the varying  $n$  value in case of the investigations by Kim et al. [62,65] compared to the constant  $n$  value used by van Bohemen [59]. However, considering the accelerating effect of the prior martensite on the isothermal transformation kinetics of bainite, a standard JMAK analysis cannot simply describe the decomposition of the remaining austenite when a fraction of martensite is already present before the isothermal transformation starts. Kim et al. assumes that the fraction of isothermal product increases from 0 to 1 for each temperature below  $M_s$ , thus independent of the fraction of remaining austenite available for transformation. Although not explicitly mentioned, the fraction of the isothermal product could be assumed as normalised in Kim et al.’s work and therefore the approach ignores any effect of the prior martensite on the isothermal transformation kinetics. Unlike Kim et al., van Bohemen et al. translated the time data instead of scaling the fraction data. They kept



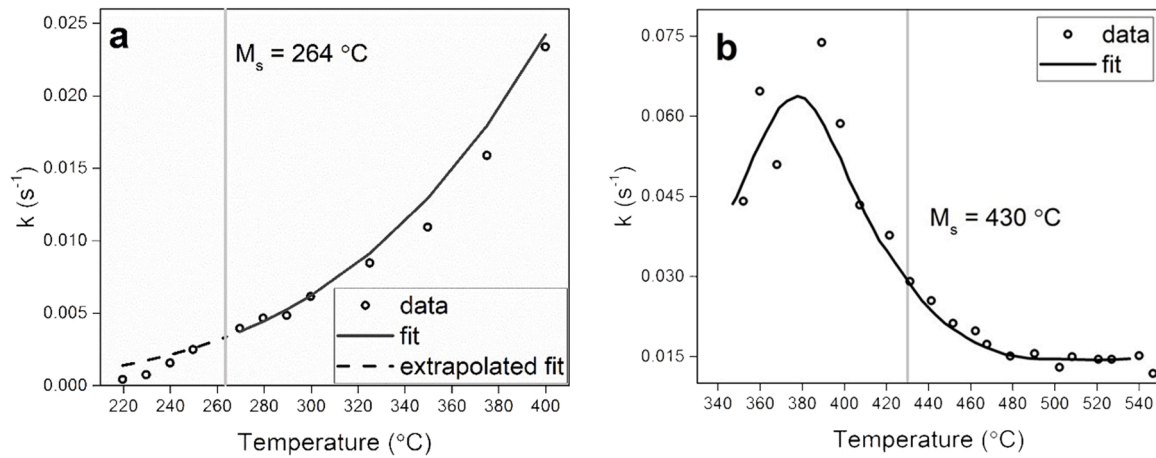


**Fig. 6.** The rate constant  $k$  values plotted as a function of temperature (a) data from van Bohemen et al. [59]; the solid line is the fit using Eq. 2 above the  $M_s$  temperature and the dashed line is the extrapolation of the fit below the  $M_s$  (b) data from Kim et al. for a 0.2 C-1.5Mn-1.5Si (wt%) steel [65].

the Avrami exponent  $n$  to be constant ( $n = 2$ ) throughout, calculated using the bainite reaction data above the  $M_s$  [59]. This approach implicitly assumes that a fraction of prior martensite in the austenite matrix has an effect on the subsequent isothermal reaction, analogous to the effect of an equal fraction of bainite. The latter, however, requires a (supposed) time duration to form below  $M_s$ , whereas the martensite is formed very fast (immediate). The analysis of van Bohemen et al. is consistent with the methodology of Howard and Cohen to display the transformation kinetics below  $M_s$  in a TTT diagram as the sum of martensite and bainite. However, the effect of prior martensite and bainite on the subsequent isothermal reaction may not be the same (an example could be found in reference [76]) and therefore an approach more sophisticated than a JMAK equation is required for modelling the effect of prior martensite on the isothermal kinetics.

Although the kinetics of the isothermal transformations below the  $M_s$  temperature show similarities with those observed above  $M_s$  as reported by various researchers, the mechanisms leading to the initial acceleration of isothermal kinetics below  $M_s$  are still under discussion. It was pointed out before that the additional nucleation sites provided by the austenite/martensite interfaces [17,18] and the transformation strains [17,19] as a result of the prior martensite formation could be the reasons for the accelerating effect. Howard and Cohen (1948) suggested the possibility of both the factors acting simultaneously; however based on their observation that the bainite units were located away from the primary martensite laths, they suggested that the deformation strains generated in the austenite during the martensitic reaction were the primary reason for acceleration [17]. However, no further discussions were made on how the conclusion is reached. Elmeendorf (1944) also hypothesized a similar conclusion although no microstructural evidence was given [19]. He reasoned that in high carbon steels the martensitic transformation would result into higher strains in the austenite and therefore comparatively faster transformation rates in higher carbon steels are expected compared to that in low carbon steels [19]. Amongst recent investigations, Toji et al. (2016) reported the bainite units formed slightly away from the martensite laths in a Si-containing steel and proposed similar reason for the acceleration [24]. Using atom probe tomography, they observed that the austenite carbon concentration near the interface is higher than the  $T_0$  point, the maximum carbon concentration for austenite to transform to bainite according to the displacive mechanism [24]. As a result, bainite formed slightly away from the prior martensite [24]. They further proposed that bainite will form at the carbon depleted regions in austenite such as near carbides [24].

### 2.3.2. Literature on transformation strains as cause for the acceleration

In an investigation of an ultrafine-grained bainitic steel, Guo et al.

(2019) reported that prior martensite plates/laths and surrounding bainite sub-units shared a common crystallographic orientation [74]. They suggested that the deformation in the austenite grains caused by the martensitic transformation may deflect the orientation of the austenite, in turn influencing the growth direction of the bainite laths and therefore the orientation of the bainite units could be regulated by the surrounding martensite [74]. Based on this, they further proposed that the strains developed during the prior martensite formation were the primary reason for the acceleration of the bainite formation kinetics [74].

In general, prior plastic deformation of austenite may greatly influence the subsequent martensite and bainite formation [77–82]. Prior straining such as ausforming increases the mechanical stability of austenite and therefore is known to lower the  $M_s$  temperature of the steel [77,78]. The effect of ausforming on the bainite kinetics depends on the level of strain and ausforming temperature and steel composition. Prior plastic deformation in austenite retarded the bainite kinetics as well as its overall volume fraction at larger strains [83,84]. Some investigators observed an initial acceleration in the kinetics that eventually became slower at the final stage [80,85–88]. In contrast to both, Gong et al. (2010–13) reported the acceleration of bainite kinetics throughout the transformation as a result of a small amount of prior ausforming (Fig. 7) [81,82]. They suggested the partial dislocations introduced in the austenite during ausforming caused the acceleration [82]. As the martensitic reaction is also able to introduce dislocations in the

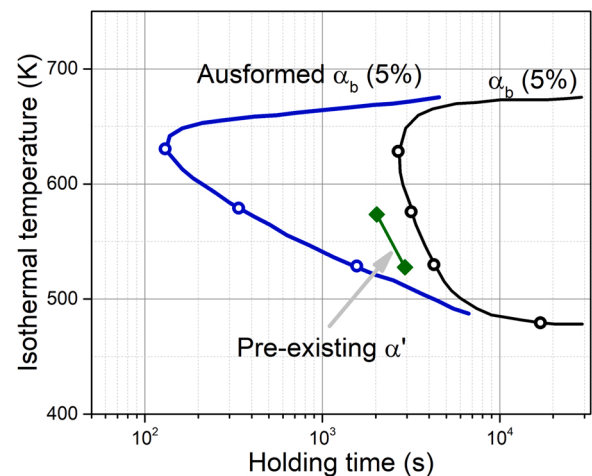


**Fig. 7.** Comparison of the effect of ausforming and prior martensite formation on the proceeding bainite formation [21].

surrounding austenite [44,45], they reasoned that the similar accelerating effect on the bainite kinetics (as of due to ausforming) is possible in the presence of martensite [21]. However, the extent of the acceleration is significantly higher for ausforming (Fig. 7). Probably, this difference is related to the distribution of dislocations. With ausforming the dislocations are uniformly distributed in an austenite grain which contrasts the more localised dislocation structure around the interfaces in case of martensite formation [21].

On the contrary, Hu et al. (2020) observed a delayed onset of bainite reaction below the  $M_s$  with a prior deformation, also below the  $M_s$ , in a medium carbon bainitic steel [79]. Increased martensite fraction further delayed the onset of bainite formation. These results contrasts the findings by Zhao et al. (2019) who compared the effect of prior ausforming (performed above the  $M_s$ ) on the subsequent bainite formation both, above and below the  $M_s$  temperature in a low carbon bainitic steel [75]. Zhao et al. concluded that combination of ausforming at a low temperature (above  $M_s$ ) and isothermal treatment below the  $M_s$  temperature is the most favourable condition for accelerated bainite kinetics and a refined microstructure. They further suggested that the acceleration in the bainite kinetics is a combined effect of the presence of martensite as well as deformation strains in austenite due to ausforming [75]. Since Hu et al. applied the plastic deformation at a temperature below the  $M_s$ , the matrix was a mixture of martensite and austenite instead of a primary austenite matrix in the investigation by Zhao et al. The co-deformation of martensite will therefore further strain the surrounding austenite, resulting in large misorientation gradients in the microstructure. Hu et al. argued that the bainite formation will be hindered at larger strains, nullifying the accelerating effect of the prior martensite on the bainite kinetics. However, more investigations are necessary to confirm the negative effect of matrix plastic deformation below the  $M_s$  on the subsequent bainite formation.

From the above discussed investigations, it could be deduced that the dominating mechanism for accelerated bainite formation is local carbon depletion in austenite regions nearby dislocations which are enriched in carbon. In addition, local strains may also play a role. However, since the strains are highest at the interface, a purely strain-induced nucleation mechanism cannot explain that the bainite laths are observed away from the interface.

Goodenow et al. (1965) [89] had a similar view about the effect of dislocations generated as a result of a prior transformation. Although their investigation included the dislocations formed as a result of prior bainite formation [89], the conclusions should also be valid for the cases with prior martensite. They attempted to eliminate the dislocations resulting from a prior bainitic transformation by performing annealing treatment above the  $B_s$  temperature [89]. Their results reveal that the bainitic transformation kinetics was significantly slower in a relaxed structure compared to that in a structure without any annealing [89]. As the dislocations were annihilated after annealing, the local carbon depletion areas were also removed. This suggests the transformation strains are the primary reasons for the acceleration.

### 2.3.3. Literature on martensite/austenite interfaces as cause of the acceleration

An increase in the number density of potential nucleation sites as a result of austenite/prior martensite interfaces was also cited as the primary reason for the acceleration by some researchers [22,23]. Kawata et al. (2010) investigated the effect of both the deformation strains and the austenite/prior martensite interfaces on the bainite kinetics by introducing polygonal ferrite and athermal martensite as the pre-existing constituents and reported that the bainite formation kinetics was similar in their steels containing 26% polygonal ferrite and 22% athermal martensite, respectively [23]. They also reported that the bainite units were formed at the interface between the martensite laths and austenite [23]. From these observations they concluded that the austenite/prior martensite interfaces were the primary nucleation sites for the bainite units [23]. An accelerated bainite kinetics in the presence

of ~10% polygonal ferrite was also reported by Quidort and Brechet (2001) for a 0.5 wt% C steel [90]. They suggested the possibility of bainitic sub-units growing from the already formed ferrite surrounding the austenite grain boundaries, without a nucleation event, thus accelerating the kinetics [90]. Similar observations were made by Ravi et al. (2020) for a low carbon Si containing steel [91]. In contrast, Zhu et al. (2013) reported that the bainitic transformation was inhibited in presence of pre-existing ferrite [92]. They proposed that the bainite kinetics is controlled by the competition between the accelerating effect of additional nucleation sites provided by the ferrite/austenite interphase boundaries and the retarding effect of increased alloying concentration (C, Mn) near the interface, introduced in austenite during prior ferrite formation [92].

$$n_{sites}(t_i) = \left( \frac{dN}{dt} \right)_{t_i} \cdot V'_{grain} \quad (4)$$

Navarro-López et al. (2016) calculated the number of potential nucleation sites per second and austenite grain ( $n_{sites}$ ) for the bainite units both above and below the  $M_s$  temperature using the following relationship [22],

where  $t_i$  is the time elapsed since the initiation of the bainite formation,  $n_{sites}$  is the number of nuclei forming per second at  $t_i$ ,  $\left( \frac{dN}{dt} \right)_{t_i}$  is the nucleation rate at  $t_i$  and  $V'_{grain}$  is the average volume of the austenite grain. Assuming the austenite grain boundaries and austenite/martensite were the only interfaces acting as the potential nucleation sites at the beginning of the isothermal transformation, Navarro-López et al. suggested that the difference in the  $n_{sites}$  value between the above and below  $M_s$  transformation cases could be attributed to the austenite/martensite interfaces [22]. They did not explicitly consider the effect of the dislocations formed during the martensite formation. Reasoning that the difference in the  $n_{sites}$  value increased with the increase in the martensite volume fraction, they suggested that the austenite/martensite interfaces were the primary sites for the bainite nucleation [22]. Hasan et al. (2020) also reported acceleration of the initial bainite nucleation rate in presence of prior martensite [76]. Based on their observation of the nucleation rate being maximum at the start of the bainite formation, they suggested that the acceleration was a result of the increase in the nucleation site density in the form of austenite/martensite interfaces [76].

### 2.3.4. Discussion on possible acceleration mechanisms

From the above discussion it is clear that the prior martensite formation has an active influence in the acceleration of the bainite kinetics although the exact mechanism is unclear. It is understood that the increase in the potential nucleation sites for bainite formation is the primary reason for acceleration, although it is not clear whether the bainite formation occurs at the austenite/prior martensite interfaces or close to the interfaces. In both the cases, the number density of interfaces is important and it seems plausible that both the factors act simultaneously, therefore complicating the analysis. For example, Navarro-López et al. [22] observed a significance increase in the bainite kinetics (about 3.5 times compared to the bainite formation above  $M_s$ ) in a steel containing only about 4% prior martensite. Therefore, the question arises whether the dislocations or the increase in austenite/martensite interfaces generated by that small fraction of martensite is indeed enough to cause a significant acceleration. For comparison purpose, the time to achieve about 34% bainite are listed in Table 2 at different investigations concerning bainite formation without and with martensite, investigated by Kawata et al. [23] and Gong et al. [21]. The volume fraction of bainite (34%) is chosen to ensure enough bainite formation and easier data extraction from the plots supplied in the corresponding investigations. The bainite fraction ( $f_B$ ) is normalised according to the method used by Kawata et al. ( $f_{B(normalised)} = f_{B(experimental)} / (1 - f_{PM})$ ,  $f_{PM}$ : prior martensite fraction) [23]. As can be seen, the transformation accelerated by only 1.5 times in the investigation by Gong et al. [21] for

**Table 2**

Comparison of acceleration in the kinetics observed in different investigations (Time: the time to reach 34% bainite (normalised), NM: no prior martensite and PM: prior martensite).

author	Composition, wt%	Isothermal temperature	$f_{PM}$	Time, s (NM)	Time, s (PM)	Acceleration factor (NM/PM)
Gong et al. [21]	0.79 C-1.98Mn-1.51Si-0.98Cr-0.24Mo-1.06Al-1.58Co	300 °C	0.06	5735.5	3758.7	1.5
Kawata et al. [23]	0.4 C-2.49Mn-0.01Si-0.03Al	320 °C	0.20	220.4	120.5	1.8

a steel containing 6%  $f_{PM}$ . In the case of Kawata et al. [23], the  $f_{PM}$  is even higher, albeit the acceleration factor is only slightly higher than Gong et al. Although there are differences in the steel compositions, the density of potential nucleation sites (either as a result of transformation strains or austenite/martensite interfaces) is expected to rise with increasing the prior martensite fraction and so the bainite kinetics. However, it should be noted that the transformation strains are likely generated at/near the austenite/martensite interfaces and therefore the quantification of the density of nucleation sites alone may not be ideal for the identification of the primary mechanism. Additionally, a definite quantitative measure of the acceleration is difficult. For example, the bainite fraction has been normalised in Table 2 in order to account for the prior martensite fraction and therefore the acceleration measured is somewhat relative in nature. With this method it is difficult to compare the absolute acceleration in the kinetics. As Toji et al. indicated, the bainite nucleation occurred at the carbon-depleted regions in austenite [24], which could be near carbides as well as near dislocations and interfaces, possibly the bainite formation is regulated by the density of carbon-depleted regions in austenite. Therefore, the above mentioned mechanisms are likely interlinked, complicating the analysis. Still, establishing a relationship between  $f_{PM}$  and the bainite kinetics at the initial stages of transformation could be helpful in understanding the mechanism.

Several researchers investigated the effect of the  $f_{PM}$  fraction on the bainite kinetics [19,22,23,62,74,76]. Some investigators reported a consistent increase in the bainite formation kinetics with an increase in  $f_{PM}$  [19,23,76]. In contrast, Navarro-López et al. observed that the bainite nucleation rate was not proportional to  $f_{PM}$  and suggested that as the martensite generally forms in clusters/blocks, the austenite/martensite interfaces were not uniformly distributed and therefore the relationship is not linear [22]. The nucleation rates calculated at 0.5 s into the reaction for the investigations by Navarro-López et al. [22] and Hasan et al. [76] are plotted in Fig. 8. The data trends seem different in the two investigations, although the investigators used the same model [93] for calculating the nucleation rate. It should be noted that there are some differences in the two investigations; 1) the steel compositions are different and 2) the isothermal temperatures in ref [22] were same as the

quenching temperatures, ranging between 320 and 270 °C, whilst in ref [76], the isothermal temperature was fixed at 430 °C, higher than the quenching temperatures. Therefore the effect of undercooling on the bainite formation kinetics could be different in both the cases. Navarro-López et al. suggested that at the initial stage the influence of the increase in the nucleation site density caused by the austenite/martensite interfaces is stronger on the kinetics than that due to the undercooling [22]. Although a sort of saturation in the nucleation rate at higher  $f_{PM}$  could be observed, the number of data points seems insufficient to establish a conclusive trend in both the cases. A systematic investigation is therefore necessary to establish the relationship between the  $f_{PM}$  and the bainite kinetics.

Kim et al. also studied the effect of  $f_{PM}$  on the isothermal transformation kinetics in low C steels containing Mn, Si and Al although they assumed the isothermal transformation product being martensitic [62–65] (refer section 2.1.2). They analysed the isothermal transformation rate as a function of the  $f_{PM}$  and observed an initial increase in the transformation rate at lower  $f_{PM}$  [62]. The increased transformation rate at lower  $f_{PM}$  was thought to be the result of the autocatalytic nucleation on the stress/strain field produced in austenite during the primary martensitic reaction [62].

### 2.3.5. Influence of prior austenite grain size

The condition of austenite, such as prior austenite grain size (PAGS), prior deformation, austenite chemical composition (including micro-alloying elements) and strength of austenite, greatly influences the subsequent martensite and bainite formation. The effect of ausforming (i.e. plastic deformation of austenite) on bainite formation in presence of martensite has been discussed previously. Prior austenite grain size influences the number density of potential grain boundary nucleation sites available for further transformation. Therefore, the nucleation events for both martensite and bainite could be partly controlled by changing the PAGS. It is known that finer PAGS lowers both the  $M_s$  and  $B_s$  temperature of a steel [94–96]. It was suggested that strengthening of austenite due to grain refinement hinders the plastic accommodation of austenite, required for the shear strain associated with martensite formation [97]. The  $M_s$  temperature is sensitive to the change of PAGS up to critical grain diameter  $D_c$  [49,50,94]. For  $PAGS > D_c$ , the grain size effect on the  $M_s$  is negligible. Van Bohemen and Morsdorf suggested that the lath aspect ratio increases below  $D_c$  [51], so the stored energy of austenite, resulting into more equiaxed laths. Therefore larger driving force is required for lath formation below  $D_c$ , lowering the  $M_s$  temperature. As the  $M_s$  is lowered, small fraction of prior martensite is expected to form at a fixed pre-quench temperature compared to that formed in a steel with coarse PAGS at the same temperature [98]. Therefore, the designing of heat treatments with prior martensite should consider the effect of PAGS. The packet size and block width of a lath martensitic structure is proportional to the PAGS [99,100]. Celada-Casero et al. have also shown that in a Q&P steel, higher density of martensite/austenite interfaces and higher carbon partitioning rate ensures a faster austenite stabilisation in smaller PAGS compared to that in larger PAGS [98]. The increased number density of martensite/austenite interfaces also may act as additional nucleation sites for subsequent bainite formation due to lower PAGS.

The bainite formation itself is also influenced by the PAGS; however, variable results are reported on its effect on the bainite formation, perhaps due to the complex nature of the transformation process. Some investigators report an accelerated bainite kinetics with decreasing

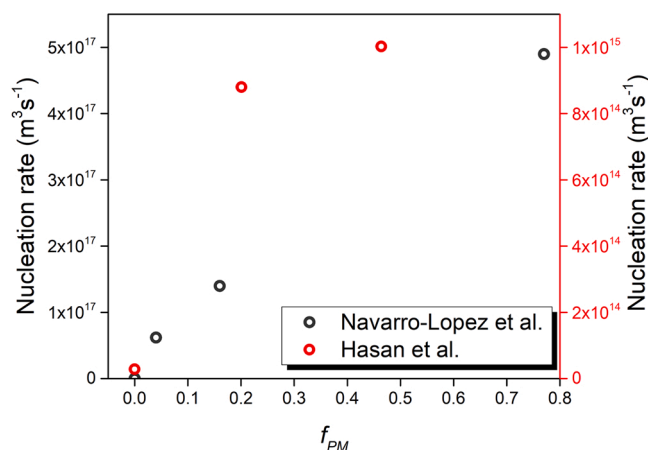


**Fig. 8.** Effect of prior martensite volume fraction on the bainite nucleation rate; comparison of the data from Navarro-López et al. [22] and Hasan et al. [76]. The nucleation rate calculated at 0.5 s into the transformation.

PAGS [93,96,101,102]; higher grain boundary area per unit volume of austenite leading to an increased nucleation rate of bainitic units. However, many argued that the growth of the bainitic units will be limited due to finer PAGS, leading to a slower overall kinetics [103,104]. Hu et al. (2014) and Hasan et al. (2020) reported the bainite formation kinetics becomes faster with increasing PAGS [105,106]. Matsuzaki and Bhadeshia (1999) proposed that the effect of PAGS on the overall bainite kinetics is dependent on the rapidness of the growth of the bainitic units; with faster growth rate, the overall kinetics becomes slower, while a slower growth rate enhances the overall kinetics with decreasing PAGS [107]. Tian et al. (2019) investigated the effect of austenitising temperature (and therefore PAGS) on the isothermal transformation below the  $M_s$  temperature in a low C steel containing Mn, Si, Mo and Cr [73]. They suggested that the bainite formation below the  $M_s$  temperature at various PAGS is dependent on the competition between the extra nucleation sites formed as a result of prior martensite formation and a decrease in nucleation sites due to larger PAGS. The volume fraction of prior martensite in itself plays a role in varying the number density of nucleation sites for bainite formation. Also, the volume fraction of prior martensite could be proportional to PAGS as discussed above. These interrelated factors make the interpretation of the effect of PAGS on the bainite formation below the  $M_s$  temperature complex and therefore must be analysed with careful consideration to the effect of PAGS on both the martensite and bainite formation. As the PAGS influences the volume fraction of both martensite and bainite, it could be used to control the amount of retained austenite at RT. The stability of the austenite should also be considered. Finer PAGS essentially limits the amount of bainite to be formed at a fixed temperature, increasing the volume fraction of remaining austenite. Additionally, the remaining austenite may become enriched with carbon due to martensite tempering and bainite formation, stabilising the austenite against brittle fresh martensite formation during cooling to RT after isothermal treatment. Yao et al. (2021) have obtained more retained austenite with finer PAGS, effectively improving the mechanical properties of a low C steel containing Mn, Si, Cr, V, Ni and Mo [108]. However, it should be noted that since finer PAGS limits the volume fraction of bainite, the remaining austenite may not become completely stabilised to avoid fresh martensite formation. The effect of PAGS on the bainite formation in presence of martensite is a rarely explored area in the literature to date. More investigations in this topic is necessary for meaningful conclusions.

### 2.3.6. Influence of chemical composition

Steel composition is also an important factor to consider as various alloying elements act differently to the stability of austenite against different phase transformations. In the present area of discussion, many researchers focused on the bainite formation in presence of prior martensite and therefore used alloying elements such as Mn, Mo and Cr, that increased the stability and hardenability of supercooled austenite so that other transformation products such as ferrite and pearlite could be avoided and the temperature range of bainitic transformations increase. Some investigators also added a combination of Co and Al, in order to improve the bainite formation at lower temperatures (such as below  $M_s$ ) by reducing the incubation time and increasing the driving force for bainite formation [21,61,109]. Si is often added in order to avoid carbide formation is austenite, thereby improving the carbon enrichment and thus stability of austenite at RT [21,22,24,74]. Some investigators also added Al in combination with Si for the same reason [21,74]. The effect of microalloying elements such as Ti, V and Nb in this kind of steels could be interesting. These elements are known to form carbides that may refine the PAGS on the event the precipitate dissolution temperature is not reached [110] and therefore both the martensite and bainite structure will be refined. In addition, austenite could be strengthened through grain boundary strengthening and precipitation hardening leading to increased volume fraction of retained austenite [111,112]. However, the carbon content of the retained austenite may decrease because of the carbide precipitates [111,112], in turn

increasing the driving force for bainite formation. The alloy carbides themselves may act as potential nucleation sites, thereby potentially increasing the kinetics of subsequent transformations. However, it is well known that all these microalloying elements (Ti, Mo, V and Nb) increase the hardenability and therefore decrease the kinetics of bainite formation. The overall rate of bainite formation will therefore depend on the dominating factor of the above discussed points. Although the effect of microalloying elements on the Q&P process has been studied by a number of researchers [111–116], their effect on the bainite formation in presence of martensite is largely understudied and therefore more investigations are necessary.

In addition to the prior austenite condition, the martensite and subsequent bainite formation is also influenced by microstructure heterogeneity caused by segregation of substitutional alloying elements such as Mn. Microstructure banding caused by alloying element segregation is often encountered in industrial steels. Both the  $M_s$  and the  $B_s$  temperature may locally differ depending on the local variation of chemical composition, further complicating the assessment of bainite formation in presence of martensite. Navarro-López et al. (2016) encountered with microstructure banding caused by Mn segregation in his investigation of bainite formation in a low C-Mn-Si-Mo steel [22]. They suggested that the  $M_s$  temperature will locally vary with the local chemical variation, leading to formation of martensite first at the Mn-poor regions compared to that at the Mn-rich regions [22]. The later regions will also be more resistant to bainite formation due to their increased austenite stability. Ravi et al. have shown that both bainite nucleation and growth are retarded by Mn-rich areas [117]. Therefore, bainite will form first at the Mn-poor areas. The severity of banding however reduces as the undercooling increases [117]. Ravi et al. argued that the increased driving force due to increased undercooling outweighs the small changes in driving force between Mn-rich and Mn-poor areas, thereby reducing the banding effect [117]. However, accounting the effect of microstructure banding is complex in distinguishing a clear mechanism for accelerating bainite kinetics.

In summary, it is possible that the accelerating effect on the isothermal transformation kinetics is caused by the increased nucleation site density in the form of both the austenite/martensite interfaces and the dislocations formed in austenite due to the prior martensite formation. The effect of other pre-existing phases such as polygonal ferrite and bainite on the subsequent isothermal kinetics in comparison to that of martensite has not been systematically investigated, although such comparison could be interesting in order to identify the dominant mechanism for acceleration. Only one study compared both the effects of prior martensite and bainite on the subsequent bainite formation kinetics and they reported the accelerating effect of the prior bainite on the isothermal transformation kinetics is comparatively lower than that of martensite [76]. This suggests that the role of the dislocations in the untransformed austenite could be dominating over the prior phase/austenite interfaces. However, the close proximity of the austenite/martensite interfaces and the dislocations in austenite generated during the martensite formation makes it difficult to distinguish a clear mechanism. In addition, consideration of factors such as PAGS, prior deformation of austenite and its chemical composition, microstructure heterogeneity due to chemical segregation, may further complicate the process.

### 3. Summary

The isothermal heat treatment in presence of prior martensite may result into the decomposition of the remaining austenite into either isothermal martensite and/or bainite, in both hypoeutectoid and hypereutectoid steels. Both isothermal products are assumed to have their own characteristic thermodynamic conditions for nucleation and growth. This means that for certain alloying compositions both bainite and isothermal martensite can in principle form in a particular temperature range. The competing reactions will have different



transformation kinetics and that determines which product is observed. Isothermal martensite formation has been reported in high carbon steels mostly. On the other hand, bainite has been observed in the presence of martensite for alloys with various carbon levels. Sometimes the bainite formation was reported to be preceded by isothermal martensite.

The bainite kinetics was found to be accelerated in the presence of the martensite, the reason is thought to be the increase in the density of nucleation sites for the isothermal product as a result of the martensitic transformation before the isothermal treatment. However, the location of bainite could not be clearly distinguished; whether at the austenite/prior martensite interfaces or close to the interfaces. Further, the possibility of both the factors acting simultaneously complicates the analysis as in both the cases the number density of interfaces is an important aspect.

There is no proper reference to judge whether the isothermal martensite formation kinetics is also accelerated in presence of athermal martensite. The strained austenitic matrix as well as the austenite/martensite interfaces serve as potential nucleation sites for the isothermal product. Whilst most of the researchers thought the deformation strains in austenite generated by the martensitic reaction is the profound contributor to the increased nucleation site density, in the absence of the direct experimental evidence, the primary factor contributing to the acceleration is still under discussion. The experimental methods proposed by Goodenow et al. [89] for eliminating dislocations introduced by the prior bainite formation could be useful in this context. Investigation of the isothermal kinetics after the elimination of dislocations in the untransformed austenite introduced by the prior martensite formation could then be able to make a distinction between the effect of new interfaces and the combined effect of dislocations and new interfaces on the isothermal kinetics. Also, the formation of martensite introduces both plastic and elastic strains in the surrounding austenite. The internal stresses due to the martensite formation is accommodated by slip and/or twinning in the martensite and slip in the surrounding austenite near the interface [44,118]. The secondary accommodation involves formation of misfit dislocations caused by both plastic and elastic strains [118]. The above investigations however did not distinguish between the contribution of the plastic or elastic component of the martensitic transformation strains on the bainite formation. Gong et al. mentioned that the thickness of the bainite area surrounding the prior martensite zone is equal to the plastic zone near a lenticular martensite plate, suggesting the role of dislocations near the interface and therefore possibly the relationship of the plastic strains and bainite formation [21]. However, the possible role of elastic strains in the austenite introduced due to prior martensite formation on the bainite formation has not been investigated. Further, effect of various factors related to the condition of austenite such as PAGS, austenite chemical composition and prior deformation are rarely explored in the literature, although those may also play a role in the formation of prior martensite as well as isothermal transformation kinetics. There is more room for investigation in this subject so to establish the nature of the isothermal product as well as the primary mechanism leading to the acceleration of the isothermal transformation kinetics.

#### CRediT authorship contribution statement

**Sharmsitha Dhara:** Conceptualization, Formal analysis, Visualization, Writing – original draft preparation. **Stefan van Bohemen:** Writing – review & editing, Supervision. **Maria J. Santofimia:** Writing – review & editing, Supervision, Funding acquisition.

#### Declaration of Competing Interest

The authors declare that they have no known competing financial interests or personal relationships that could have appeared to influence the work reported in this paper.

#### Data availability

This is a review article. The data used in this article has been taken from the literature.

#### Acknowledgements

The research was carried out under the project number T18005 in the framework of the Research Program of the Materials innovation institute (M2i) ([www.m2i.nl](http://www.m2i.nl)) supported by the Dutch government. The support of Tata Steel to this project is acknowledged.

#### References

- [1] V.F. Zackay, E.R. Parker, D. Fahr, R. Busch, The enhancement of ductility in high-strength steels, *ASM Trans. Quart.* 60 (2) (1967) 252–259.
- [2] H.K.D.H. Bhadeshia, D.V. Edmonds, Bainite in silicon steels: new composition–property approach Part 1, *Met. Sci.* 17 (9) (1983) 411–419.
- [3] J. Speer, D.K. Matlock, B.C. De Cooman, J.G. Schroth, Carbon partitioning into austenite after martensite transformation, *Acta Mater.* 51 (9) (2003) 2611–2622.
- [4] E.R. Morgan, T. Ko, Thermal stabilization of austenite in iron-carbon-nickel alloys, *Acta Metall.* 1 (1) (1953) 36–48.
- [5] R.L. Miller, Ultrafine-grained microstructures and mechanical properties of alloy steels, *Metall. Mater. Trans. B* 3 (4) (1972) 905–912.
- [6] Y.K. Lee, J. Han, Current opinion in medium manganese steel, *Mater. Sci. Technol.* 31 (7) (2015) 843–856.
- [7] J. Speer, R. Rana, D. Matlock, A. Glover, G. Thomas, E. De, Moor, Processing variants in medium-Mn steels, *Metals* 9 (7) (2019) 771.
- [8] F.G. Caballero, H.K.D.H. Bhadeshia, K.J.A. Mawella, D.G. Jones, P. Brown, Design of novel high strength bainitic steels: Part 1, *Mater. Sci. Technol.* 17 (5) (2001) 512–516.
- [9] F.G. Caballero, H.K.D.H. Bhadeshia, K.J.A. Mawella, D.G. Jones, P. Brown, Design of novel high strength bainitic steels: Part 2, *Mater. Sci. Technol.* 17 (5) (2001) 517–522.
- [10] F.G. Caballero, H.K.D.H. Bhadeshia, Very strong bainite, *Curr. Opin. Solid State Mater. Sci.* 8 (3–4) (2004) 251–257.
- [11] C. Garcia-Mateo, F.G. Caballero, Ultra-high-strength Bainitic Steels, *ISIJ Int.* 45 (11) (2005) 1736–1740.
- [12] J.G. Speer, D.V. Edmonds, F.C. Rizzo, D.K. Matlock, Partitioning of carbon from supersaturated plates of ferrite, with application to steel processing and fundamentals of the bainite transformation, *Curr. Opin. Solid State Mater. Sci.* 8 (3–4) (2004) 219–237.
- [13] J.G. Speer, F.C.R. Assunção, D.K. Matlock, D.V. Edmonds, The “quenching and partitioning” process: background and recent progress, *Mater. Res.* 8 (4) (2005) 417–423.
- [14] L.C. Chang, H.K.D.H. Bhadeshia, Carbon content of austenite in isothermally transformed 300M steel, *Mater. Sci. Eng.: A* 184 (1) (1994) L17–L19.
- [15] H.K.D.H. Bhadeshia, A.R. Waugh, Bainite: An atom-probe study of the incomplete reaction phenomenon, *Acta Metall.* 30 (4) (1982) 775–784.
- [16] M.J. Santofimia, S.M.C. van Bohemen, J. Sietsma, Combining bainite and martensite in steel microstructures for light weight applications, *J. South. Afr. Inst. Min. Metall.* 113 (2013) 143–148.
- [17] R. Howard, M. Cohen, Austenite transformation above and within the martensite range, *Trans. AIME* 176 (3) (1948) 4.
- [18] S. Radcliffe, E. Rollason, The kinetics of the formation of bainite in high-purity iron-carbon alloys, *J. Iron Steel Inst.* 191 (1959) 56–65.
- [19] H. Elmdendorf, The effect of varying amounts of martensite upon the isothermal transformation of austenite remaining after controlled quenching, *Trans. ASM* 33 (1944) 236–254.
- [20] E. Pinto da Silva, W. Xu, C. Föjer, Y. Houbaert, J. Sietsma, R.H. Petrov, Phase transformations during the decomposition of austenite below Ms in a low-carbon steel, *Mater. Charact.* 95 (2014) 85–93.
- [21] W. Gong, Y. Tomota, S. Harjo, Y.H. Su, K. Aizawa, Eff. Prior. martensite bainite Transform. nanobainite Steel 85 (2015) 243–249.
- [22] A. Navarro-López, J. Sietsma, M.J. Santofimia, Effect of Prior Athermal Martensite on the Isothermal Transformation Kinetics Below Ms in a Low-C High-Si Steel, *Metall. Mater. Trans. A* 47 (3) (2016) 1028–1039.
- [23] H. Kawata, K. Hayashi, N. Sugiura, N. Yoshinaga, M. Takahashi, Effect of Martensite in Initial Structure on Bainite Transformation, *Mater. Sci. Forum* 638–642 (2010) 3307–3312.
- [24] Y. Toji, H. Matsuda, D. Raabe, Effect of Si on the acceleration of bainite transformation by pre-existing martensite, *Acta Mater.* 116 (2016) 250–262.
- [25] M. Morawiec, V. Ruiz-Jimenez, C. Garcia-Mateo, J.A. Jimenez, A. Grajcar, Study of the isothermal bainitic transformation and austenite stability in an advanced Al-rich medium-Mn steel, *Arch. Civ. Mech. Eng.* 22 (4) (2022) 152.
- [26] H. Bhadeshia, R. Honeycombe, *Steel: Microstruct. Prop.* (2006).
- [27] A.R. Entwistle, The kinetics of martensite formation in steel, *Metall. Trans.* 2 (9) (1971) 2395–2407.
- [28] J.C. Bokros, E.R. Parker, The mechanism of the martensite burst transformation in Fe-Ni single crystals, *Acta Metall.* 11 (12) (1963) 1291–1301.
- [29] A. Borgenstam, M. Hillert, Activation energy for isothermal martensite in ferrous alloys, *Acta Mater.* 45 (2) (1997) 651–662.

- [30] C. Shih, B. Averbach, M. Cohen, Some characteristics of the isothermal martensitic transformation, *JOM* 7 (1) (1955) 183–187.
- [31] R. Cech, J. Hollomon, Rate of formation of isothermal martensite in Fe-Ni-Mn alloy, *Trans. Am. Inst. Min. Metall. Eng.* 197 (5) (1953) 685–689.
- [32] G. Kurdjumov, O. Maksimova, Kinetics of austenite to martensite transformation at low temperatures, *Dokl. Akad. Nauk SSSR* 61 (1) (1948) 83–86.
- [33] S.R. Pati, M. Cohen, Kinetics of isothermal martensitic transformations in an iron-nickel-manganese alloy, *Acta Metall.* 19 (12) (1971) 1327–1332.
- [34] B. Averbach, M. Cohen, The isothermal decomposition of martensite and retained austenite, *Transactions of the American Society for Metals* 41 (1949) 1024–1060.
- [35] H. Okamoto, M. Oka, Isothermal martensite transformation in a 1.80 wt Pct C steel, *Metall. Trans. A* 16 (12) (1985) 2257–2262.
- [36] H. Okamoto, M. Oka, Lower bainite with midrib in hypereutectoid steels, *Metall. Trans. A* 17 (7) (1986) 1113–1120.
- [37] M. Oka, H. Okamoto, Swing back in kinetics near Ms in hypereutectoid steels, *Metall. Trans. A* 19 (3) (1988) 447–452.
- [38] M. Lin, G.B. Olson, M. Cohen, Distributed-activation kinetics of heterogeneous martensitic nucleation, *Metall. Trans. A* 23 (11) (1992) 2987–2998.
- [39] D.P. Koistinen, R.E. Marburger, A general equation prescribing the extent of the austenite-martensite transformation in pure iron-carbon alloys and plain carbon steels, *Acta Metall.* 7 (1) (1959) 59–60.
- [40] C. Magee, The nucleation of martensite, *Phase transformations*, 1970.
- [41] R. Pradhan, G.S. Ansell, Kinetics of the martensite transformation in athermal Fe-C-Ni-Cr alloys, *Metall. Trans. A* 9 (6) (1978) 793–801.
- [42] G.B. Olson, M. Cohen, A general mechanism of martensitic nucleation: Part III. Kinetics of martensitic nucleation, *Metall. Trans. A* 7 (12) (1976) 1915–1923.
- [43] V. Raghavan, Kinetics of martensite transformations in the book *Martensite: A tribute to Morris Cohen*, edited by G.B. Olson and W.S. Owen., 1992.
- [44] G. Miyamoto, A. Shibata, T. Maki, T. Furuhara, Precise measurement of strain accommodation in austenite matrix surrounding martensite in ferrous alloys by electron backscatter diffraction analysis, *Acta Mater.* 57 (4) (2009) 1120–1131.
- [45] A. Shibata, S. Morito, T. Furuhara, T. Maki, Local orientation change inside lenticular martensite plate in Fe–33Ni alloy, *Scr. Mater.* 53 (5) (2005) 597–602.
- [46] S. Chatterjee, H.S. Wang, J.R. Yang, H.K.D.H. Bhadeshia, Mechanical stabilisation of austenite, *Mater. Sci. Technol.* 22 (6) (2006) 641–644.
- [47] S.M.C. van Bohemen, J. Sietsma, Effect of composition on kinetics of athermal martensite formation in plain carbon steels, *Mater. Sci. Technol.* 25 (8) (2009) 1009–1012.
- [48] S.M.C. van Bohemen, Bainite and martensite start temperature calculated with exponential carbon dependence, *Mater. Sci. Technol.* 28 (4) (2012) 487–495.
- [49] A. García-Junceda, C. Capdevila, F.G. Caballero, C.G. de Andrés, Dependence of martensite start temperature on fine austenite grain size, *Scr. Mater.* 58 (2) (2008) 134–137.
- [50] H.-S. Yang, H.K.D.H. Bhadeshia, Austenite grain size and the martensite-start temperature, *Scr. Mater.* 60 (7) (2009) 493–495.
- [51] S.M.C. van Bohemen, L. Morsdorf, Predicting the Ms temperature of steels with a thermodynamic based model including the effect of the prior austenite grain size, *Acta Mater.* 125 (2017) 401–415.
- [52] S. Matas, R.F. Hehemann, Retained Austenite and the Tempering of Martensite, *Nature* 187 (4738) (1960) 685–686.
- [53] K.R. Kinsman, J.C. Shyne, The thermal stabilization of austenite, *Acta Metall.* 14 (9) (1966) 1063–1072.
- [54] R.H. Edwards, The isothermal transformation of austenite at temperatures near Ms., *University of Wollongong*, 1970.
- [55] O. Schaaber, Some Observations on Isothermal Austenite Transformation Near the Ms Temperature, *JOM* 7 (4) (1955) 559–560.
- [56] G.F. Vander Voort, *Atlas of Time-temperature Diagrams for Irons and Steels*, ASM International, 1991.
- [57] E.S. Davenport, E.C. Bain, Transformation of austenite at constant subcritical temperatures, *Metall. Trans. A* 1 (12) (1970) 3503–3530.
- [58] A. Haynes, W. Steven, The temperature of formation of martensite and bainite in low-alloy steel, *J. Iron Steel Inst.* 183 (1956) 349–359.
- [59] S.M.C. Van Bohemen, M.J. Santofimia, J. Sietsma, Experimental evidence for bainite formation below Ms in Fe–0.66C, *Scr. Mater.* 58 (6) (2008) 488–491.
- [60] M.C. Somani, D.A. Porter, L.P. Karjalainen, R.D.K. Misra, On Various Aspects of Decomposition of Austenite in a High-Silicon Steel During Quenching and Partitioning, *Metall. Mater. Trans. A* 45 (3) (2014) 1247–1257.
- [61] S. Samanta, P. Biswas, S. Giri, S.B. Singh, S. Kundu, Formation of bainite below the Ms temperature: Kinetics and crystallography, *Acta Mater.* 105 (2016) 390–403.
- [62] D.H. Kim, J.G. Speer, H.S. Kim, B.C. De, Cooman, Observation of an Isothermal Transformation during Quenching and Partitioning Processing, *Metall. Mater. Trans. A* 40 (9) (2009) 2048–2060.
- [63] D.H. Kim, J.G. Speer, B.C. De, Cooman, The isothermal transformation of low-alloy low-C CMnSi steels below Ms, *Mater. Sci. Forum, Trans. Tech. Publ.* (2010) 98–101.
- [64] D. Kim, J.G. Speer, B.C. De Cooman, Isothermal Transformation of a CMnSi Steel Below the Ms Temperature, *Metall. Mater. Trans. A* 42 (6) (2011) 1575–1585.
- [65] D. Kim, S.-J. Lee, B.C. De Cooman, Microstructure of Low C Steel Isothermally Transformed in the Ms to Mf Temperature Range, *Metall. Mater. Trans. A* 43 (13) (2012) 4967–4983.
- [66] T. Waterschoot, K. Verbeken, Tempering kinetics of the martensitic phase in DP steel, *ISIJ Int.* 46 (1) (2006) 138–146.
- [67] P. Kolmskog, A. Borgenstam, M. Hillert, P. Hedström, S.S. Babu, H. Terasaki, Y.-I. Komizo, Direct Observation that Bainite can Grow Below MS, *Metall. Mater. Trans. A* 43 (13) (2012) 4984–4988.
- [68] A. Navarro-López, J. Hidalgo, J. Sietsma, M.J. Santofimia, Characterization of bainitic/martensitic structures formed in isothermal treatments below the Ms temperature, *Mater. Charact.* 128 (2017) 248–256.
- [69] N.N. Thadhani, M.A. Meyers, Kinetics of isothermal martensitic transformation, *Prog. Mater. Sci.* 30 (1) (1986) 1–37.
- [70] V. Smanio, T. Sourmail, Effect of partial martensite transformation on bainite reaction kinetics in different 1% C steels, *Solid State Phenom.* 172–174 (2011) 821–826.
- [71] I.A. Yakubtsov, G.R. Purdy, Analyses of transformation kinetics of carbide-free bainite above and below the athermal martensite-start temperature, *Metall. Mater. Trans. A* 43 (2) (2012) 437–446.
- [72] J. Tian, G. Xu, M. Zhou, H. Hu, Refined bainite microstructure and mechanical properties of a high-strength low-carbon bainitic steel treated by austempering below and above Ms, *Steel Res. Int.* 89 (4) (2018), 1700469.
- [73] J. Tian, G. Xu, Z. Jiang, Q. Yuan, G. Chen, H. Hu, Effect of austenisation temperature on bainite transformation below martensite starting temperature, *Mater. Sci. Technol.* 35 (13) (2019) 1539–1550.
- [74] H. Guo, X. Feng, A. Zhao, Q. Li, J. Ma, Influence of prior martensite on bainite transformation, microstructures, and mechanical properties in ultra-fine bainitic steel, *Mater. (Basel)* 12 (3) (2019) 527.
- [75] L. Zhao, L. Qian, Q. Zhou, D. Li, T. Wang, Z. Jia, F. Zhang, J. Meng, The combining effects of ausforming and below-Ms, or above-Ms, austempering on the transformation kinetics, microstructure and mechanical properties of low-carbon bainitic steel, *Mater. Des.* 183 (2019), 108123.
- [76] S.M. Hasan, S. Kumar, D. Chakrabarti, S.B. Singh, Understanding the effect of prior bainite/martensite on the formation of carbide-free bainite, *Philos. Mag.* 100 (7) (2020) 797–821.
- [77] E.M. Breinan, G.S. Ansell, The influence of austenite strength upon the austenite-martensite transformation in alloy steels, *Metall. Trans.* 1 (6) (1970) 1513–1520.
- [78] T.S. Wang, M. Zhang, Y.H. Wang, J. Yang, F.C. Zhang, Martensitic transformation behaviour of deformed supercooled austenite, *Scr. Mater.* 68 (2) (2013) 162–165.
- [79] H. Hu, J. Tian, G. Xu, H.S. Zurob, New insights into the effects of deformation below-Ms on isothermal kinetics of bainitic transformation, *J. Mater. Res. Technol.* 9 (6) (2020) 15750–15758.
- [80] S. Singh, H. Bhadeshia, Quantitative evidence for mechanical stabilization of bainite, *Mater. Sci. Technol.* 12 (7) (1996) 610–612.
- [81] W. Gong, Y. Tomota, M.S. Koo, Y. Adachi, Effect of ausforming on nanobainite steel, *Scr. Mater.* 63 (8) (2010) 819–822.
- [82] W. Gong, Y. Tomota, Y. Adachi, A.M. Paradowska, J.F. Kelleher, S.Y. Zhang, Effects of ausforming temperature on bainite transformation, microstructure and variant selection in nanobainite steel, *Acta Mater.* 61 (11) (2013) 4142–4154.
- [83] J.R. Yang, C.Y. Huang, W.H. Hsieh, C.S. Chiou, Mechanical Stabilization of Austenite against Bainitic Reaction in Fe-Mn-Si-C Bainitic Steel, *Mater. Trans., JIM* 37 (4) (1996) 579–585.
- [84] C.S. Chiou, J.R. Yang, C.Y. Huang, The effect of prior compressive deformation of austenite on toughness property in an ultra-low carbon bainitic steel, *Mater. Chem. Phys.* 69 (1) (2001) 113–124.
- [85] P.H. Shipway, H.K.D.H. Bhadeshia, Mechanical stabilisation of bainite, *Mater. Sci. Technol.* 11 (11) (1995) 1116–1128.
- [86] H.K.D.H. Bhadeshia, The bainite transformation: unresolved issues, *Mater. Sci. Eng.: A* 273 275 (1999) 58–66.
- [87] R. Freiwilg, J. Kudrman, P. Chráska, Bainite transformation in deformed austenite, *Metall. Trans. A* 7 (8) (1976) 1091–1097.
- [88] X.J. Jin, N. Min, K.Y. Zheng, T.Y. Hsu, The effect of austenite deformation on bainite formation in an alloyed eutectoid steel, *Mater. Sci. Eng.: A* 438 440 (2006) 170–172.
- [89] R.H. Goodenow, R.H. Barkalow, R.F. Hehemann, Bainite transformations in hypoeutectoid steels, *Iron Steel Inst. Spec. Rep.* 93 (1965) 135–141.
- [90] D. Quidort, Y.J.M. Brechet, Isothermal growth kinetics of bainite in 0.5% C steels, *Acta Mater.* 49 (20) (2001) 4161–4170.
- [91] A.M. Ravi, A. Kumar, M. Herbig, J. Sietsma, M.J. Santofimia, Impact of austenite grain boundaries and ferrite nucleation on bainite formation in steels, *Acta Mater.* 188 (2020) 424–434.
- [92] K. Zhu, H. Chen, J.-P. Masse, O. Bouaziz, G. Gachet, The effect of prior ferrite formation on bainite and martensite transformation kinetics in advanced high-strength steels, *Acta Mater.* 61 (16) (2013) 6025–6036.
- [93] S.M.C. van Bohemen, J. Sietsma, Modeling of isothermal bainite formation based on the nucleation kinetics, *Int. J. Mater. Res.* 99 (7) (2008) 739–747.
- [94] J. Fisher, J. Hollomon, D. Turnbull, Kinetics of the austenite→ martensite transformation, *JOM* 1 (10) (1949) 691–700.
- [95] L. Lan, Z. Chang, P. Fan, Exploring the Difference in Bainite Transformation with Varying the Prior Austenite Grain Size in Low Carbon Steel, *Metals* 8 (12) (2018) 988.
- [96] S.-J. Lee, J.-S. Park, Y.-K. Lee, Effect of austenite grain size on the transformation kinetics of upper and lower bainite in a low-alloy steel, *Scr. Mater.* 59 (1) (2008) 87–90.
- [97] P.J. Brofman, G.S. Ansell, On the effect of fine grain size on the Ms temperature in Fe-27Ni-0.025C alloys, *Metall. Trans. A* 14 (9) (1983) 1929–1931.
- [98] C. Celada-Casero, C. Kwakernaak, J. Sietsma, M.J. Santofimia, The influence of the austenite grain size on the microstructural development during quenching and partitioning processing of a low-carbon steel, *Mater. Des.* 178 (2019), 107847.
- [99] T. Maki, K. Tsuzaki, I. Tamura, The morphology of microstructure composed of lath martensites in steels, *Trans. Iron Steel Inst. Jpn.* 20 (4) (1980) 207–214.

- [100] S. Morito, H. Saito, T. Ogawa, T. Furuhara, T. Maki, Effect of Austenite Grain Size on the Morphology and Crystallography of Lath Martensite in Low Carbon Steels, *ISIJ Int.* 45 (1) (2005) 91–94.
- [101] J. Barford, W. Owen, The effect of austenite grain size and temperature on the rate of bainite transformation, *Met. Sci. Heat. Treat. Met* 4 (1961) 359–360.
- [102] M. Umemoto, K. Horiuchi, I. Tamura, Transformation kinetics of bainite during isothermal holding and continuous cooling, *Tetsu-to-Hagane* 68 (3) (1982) 461–470.
- [103] G. Xu, F. Liu, L. Wang, H. Hu, A new approach to quantitative analysis of bainitic transformation in a superbainite steel, *Scr. Mater.* 68 (11) (2013) 833–836.
- [104] L.W. Graham, H.J. Axon, *J. Iron, Steel Inst.* 191 (1959) 361–365.
- [105] F. Hu, P.D. Hodgson, K.M. Wu, Acceleration of the super bainite transformation through a coarse austenite grain size, *Mater. Lett.* 122 (2014) 240–243.
- [106] S.M. Hasan, S. Kumar, D. Chakrabarti, S.B. Singh, Effect of prior austenite grain size on the formation of carbide-free bainite in low-alloy steel, *Philos. Mag.* 100 (18) (2020) 2320–2334.
- [107] A. Matsuzaki, H.K.D.H. Bhadeshia, Effect of austenite grain size and bainite morphology on overall kinetics of bainite transformation in steels, *Mater. Sci. Technol.* 15 (5) (1999) 518–522.
- [108] C. Yao, H. Lan, Z. Tao, R.D.K. Misra, L. Du, Enhanced Strength and Toughness of Low-Carbon Bainitic Steel by Refining Prior Austenite Grains and Austempering Below  $M_s$ , *Steel Res. Int.* 92 (11) (2021), 2100263.
- [109] S. Samanta, S. Das, D. Chakrabarti, I. Samajdar, S.B. Singh, A. Haldar, Development of Multiphase Microstructure with Bainite, Martensite, and Retained Austenite in a Co-Containing Steel Through Quenching and Partitioning (Q&P) Treatment, *Metall. Mater. Trans. A* 44 (13) (2013) 5653–5664.
- [110] A. Karmakar, S. Kundu, S. Roy, S. Neogy, D. Srivastava, D. Chakrabarti, Effect of microalloying elements on austenite grain growth in Nb–Ti and Nb–V steels, *Mater. Sci. Technol.* 30 (6) (2014) 653–664.
- [111] G.-T. Zhang, N.-Q. Zhu, B.-W. Sun, Z.-Z. Zhao, Z.-W. Zheng, D. Tang, L. Li, Effect of V Addition on Microstructure and Mechanical Properties in C–Mn–Si Steels after Quenching and Partitioning Processes, *Metals* 11 (8) (2021) 1306.
- [112] S. Yan, X. Liu, T. Liang, J. Chen, Y. Zhao, Effect of Micro-Alloying Elements on Microstructure and Mechanical Properties in C–Mn–Si Quenching and Partitioning (Q&P) Steels, *Steel Res. Int.* 90 (1) (2019), 1800257.
- [113] J. Zhang, H. Ding, R.D.K. Misra, C. Wang, Microstructural evolution and consequent strengthening through niobium-microalloying in a low carbon quenched and partitioned steel, *Mater. Sci. Eng.: A* 641 (2015) 242–248.
- [114] S.T. Xie, Z.Y. Liu, Z. Wang, G.D. Wang, Microstructure and mechanical properties of a Ti-microalloyed low-carbon stainless steel treated by quenching-partitioning-tempering process, *Mater. Charact.* 116 (2016) 55–64.
- [115] J. Dong, X. Zhou, Y. Liu, C. Li, C. Liu, H. Li, Effects of quenching-partitioning-tempering treatment on microstructure and mechanical performance of Nb–V–Ti microalloyed ultra-high strength steel, *Mater. Sci. Eng.: A* 690 (2017) 283–293.
- [116] F. Peng, Y. Xu, X. Gu, Y. Wang, X. Liu, J. Li, The relationships of microstructure-mechanical properties in quenching and partitioning (Q&P) steel accompanied with microalloyed carbide precipitation, *Mater. Sci. Eng.: A* 723 (2018) 247–258.
- [117] A.M. Ravi, A. Navarro-López, J. Sietsma, M.J. Santofimia, Influence of martensite/austenite interfaces on bainite formation in low-alloy steels below  $M_s$ , *Acta Mater.* 188 (2020) 394–405.
- [118] D. Dunne, Martensite, *Metals* 8 (6) (2018) 395.